J. Phys. Chem. A **2008,** *112,* 2855−2862

Instability of the Al_4^{2-} “All-Metal Aromatic” Ion and Its Implications

Daniel S. Lambrecht*,† **and Timo Fleig**

Institut für Theoretische und Computerchemie, Heinrich-Heine-Universität Düsseldorf, Universitätsstr. 1, 40225 Düsseldorf, Germany

Thomas Sommerfeld

Department of Chemistry and Physics, Southeastern Louisiana University, SLU 10878, Hammond, Louisiana 70402

Received: September 13, 2007; In Final Form: January 14, 2008

Al_4^{2-} is a prototype structural unit of a new class of “all-metal aromatic” molecules. Without stabilizing counterions this species is unstable with respect to electron autodetachment in the gas phase. We estimated the height of the repulsive Coulomb barrier to approximately 2.7 eV and calculated a lifetime of 9 fs. This is a short lifetime: The only way to study the isolated dianion experimentally is to use electron scattering techniques. Investigations of the validity of bound-state quantum chemical calculations on the isolated species show that the results suffer from significant admixture of continuum states to the bound-state wave function depending on the basis set. Calculations of molecular properties can therefore give essentially arbitrary results for this ill-defined system, as is demonstrated for the energy and nuclear magnetic shieldings. This substantiates that results from calculations on the isolated dianion should be approached with caution.

I. Introduction

Recently a new kind of “all-metal aromatic” molecule MAl_4^- (M = Li, Na, K) has been discovered in laser vaporization experiments.[1] Combined theoretical and photoelectron spectroscopy (PES) investigations showed that these species contain square-planar Al_4^{2-} units with two delocalized π electrons in the highest occupied molecular orbital (HOMO).[1,2] From this it was concluded that the Al_4^{2-} units were aromatic according to the $(4n + 2)$ rule.[1] Several quantum chemical studies on Al_4^{2-} with and without counterions support this claim according to various criteria of aromaticity.[1−18] However, the isolated Al_4^{2-} is unstable to emission of one of its excess electrons (cf. refs 1 and 7) and has not yet been observed or characterized experimentally. This instability also leads to complications in quantum chemical calculations: The isolated Al_4^{2-} wave function is not a stationary eigenstate of the Schrödinger equation. Time-independent “bound-state” calculations on the isolated dianion may therefore break down if its lifetime is small.[19−22] The significance of molecular properties extracted from such calculations is then at least questionable, and conclusions drawn from them are uncertain. A more appropriate theoretical description for such cases may be obtained by taking the continuum (unbound) states $Al_4^- +$ free e^- into account.[19]

In multiply charged anions like the Al_4^{2-} under investigation here, one generally finds a repulsive Coulomb barrier (RCB), which can be understood as follows: When an excess electron is detached from the system, it encounters a short-range attraction from the nuclei and a long-range repulsion from the remaining negative charge of the system. Putting both potentials together results in a barrier, the RCB, which an electron has to overcome during its emission process. One can try to describe the bound part of the resonance wave function, that is, the part that is trapped behind the barrier, using bound-state calculations without diffuse basis functions. However, this approach can only be adequate if the energy of the state is well below the top of the barrier, in other words, if the dianion possesses a substantial lifetime. In this case adding moderately diffuse functions to the basis does not change the properties. Previous calculations on Al_4^{2-} rely on this argument. However, neither the autodetachment lifetime of the isolated dianion, nor the height of its RCB nor the influence of systematically adding diffuse functions to the basis set have been investigated.

In this article we focus on the stability and lifetime of the isolated dianion rather than following the question of aromaticity (there are many computations in the literature concerning aromaticity[1−18]). In the first place (section II) we study the height of the RCB and the lifetime of the dianion using a complex absorbing potential (CAP) combined with a configuation interaction wave function (CAP/CI). Our results suggest a very short lifetime. We therefore investigate in the second place (section III) the properties of Al_4^{2-} as a function of the diffuseness of the basis set. As expected from the short lifetime, we observe a strong basis set dependence of the computed properties.

II. Coulomb Barrier and Lifetime of Al_4^{2-}

In this section we compute the lifetime of the isolated Al_4^{2-} dianion using two approaches: First, the lifetime is estimated from the RCB. Second, the lifetime is computed using the CAP method.

Calculating an approximation to the RCB is the simplest way to characterize a metastable dianion.[21] An RCB is the potential an excess electron sees when approaching an anion (in this case a monoanion). At long range the Coulomb potential between

---

* To whom correspondence should be addressed.

† Current address: Institut f. Physikalische u. Theoretische Chemie, Eberhard-Karls-Universität Tübingen, Auf der Morgenstelle 8, 72076 Tübingen, Germany.

10.1021/jp077377c CCC: $40.75

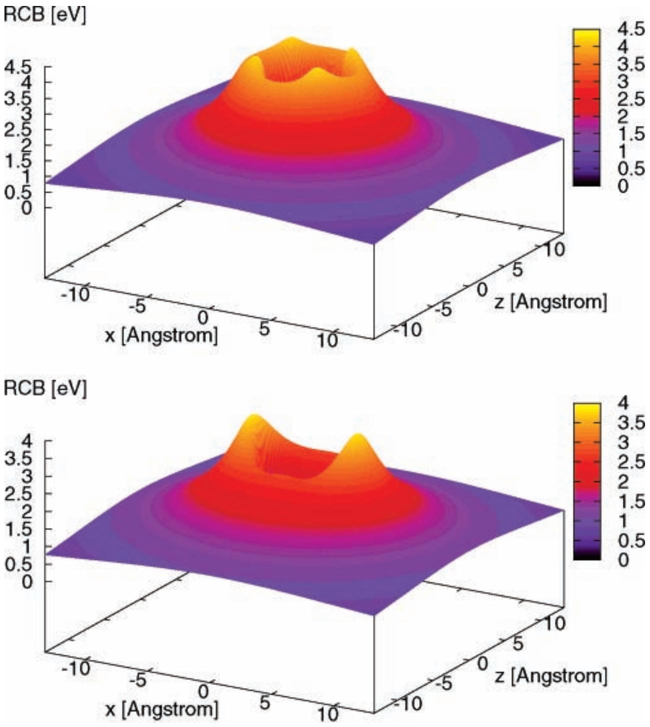

Figure 1. Cuts through the repulsive Coulomb barrier of Al_4^{2-}. The plotted local potential has been computed using the dianion frozen orbital static approximation (see text for details). The upper panel shows a cut through the molecular plane; the lower panel shows a cut orthogonal to the molecular plane through the diagonal of the Al_4 square.

the two negatively charged species is repulsive, yet at short range the attraction by the nuclei can overcome the electron−electron repulsion, giving rise to a barrier. Since Coulombic barriers are broad, even states just below the top of the barrier can have substantial lifetimes. However, Coulomb barriers are not straightforward local potentials but energy-dependent, nonlocal potentials, since at short and intermediate range the correlation between the "excess" and the "other" electrons determines the dynamics of the system. Currently there is no established method to compute the exact Coulomb barrier.[21] Nevertheless, there are different local approximations that can be very useful to compare lifetime trends in a series of closely related systems, or to roughly estimate the order of magnitude of the lifetime.

We have computed the RCB using the so-called dianion frozen orbital static approximation (DFOSA),[21] which yields a HF-like estimate of the barrier height. Two cuts through the three-dimensional DFOSA potential are shown in Figure 1. With the four-membered Al_4 in the *xy* plane, the minimal energy path above the barrier is along the *z* axis, that is, from the ring center along the direction orthogonal to the Al_4 plane. The barrier height associated with this path is 2.7 eV which is about 0.5 eV above the HOMO energy (2.2 eV) obtained with a compact basis set.[23] Thus, in view of the width of the Coulomb barrier, one could be tempted to conclude that emission from the HOMO should be slow. This is, however, deceptive. Estimating the tunneling rate using a semiclassical WKB[24] formula yields roughly 1.1 for the exponential factor, where the semiclassical lifetime is the product of the exponential factor and the frequency with which the electron impinges the barrier. Clearly, based on the DFOSA approximation one predicts a very short lifetime in the order of magnitude of the time a valence electron needs to transverse the Al_4 ring.

In order to get a more reliable estimate of the lifetime we employed the CAP/CI method that yields the Siegert energy of the resonance. The isolated Al_4^{2-} dianion represents an unstable resonance state that can be described with a complex Siegert energy

$$E_{res} = E_r - i\,\frac{\Gamma}{2} \tag{1}$$

where the real part E_r is the resonance position above the Al_4^- monoanion, and Γ is the decay width which is related to the lifetime $\tau = \hbar/\Gamma$. To compute the resonance energy we employed a complex absorbing potential (CAP) in conjunction with a configuration interaction (CI) wavefunction (CAP/CI).[25,26] The absorbing potential method[27,28] is a general and flexible technique to describe decay processes. An absorbing potential $-\mathrm{i}W$ is added to the physical Hamiltonian H, yielding a non-Hermitian complex-symmetric Hamiltonian

$$H(\eta) = H - \mathrm{i}\eta W \tag{2}$$

where η is a strength parameter. The potential W is typically a real "soft" box-like potential in the "dissociation coordinate" R, e.g., R^2 or R^4. The resonance energy E_{res} is obtained *directly* as a complex eigenvalue of $H(\eta)$, and the associated resonance wavefunction is square integrable allowing the use of regular basis set expansions. Loosely speaking, a CAP is added to the Hamiltonian to absorb the outgoing electron, and it is straightforward to combine the CAP method with existing electronic structure codes. A detailed description of general aspects of the CAP method can be found in ref 28, for the CAP/CI method see refs 25 and 26 and for similar applications see refs 29−31.

The one-particle basis set employed in the present CAP/CI calculations is Dunning's [6s5p] valence triple-ζ set[32] augmented with two d-type polarization functions (exponents 0.622 and 0.155) as well as with a 2s8p set of diffuse functions (evenly scaled exponents starting from the smallest exponents of the valence set; for the s exponents the scaling factor is 3, for the p exponents it is 1.6). This results in an [8s13p2d] atomic basis. The orbitals used to construct the CI wavefunctions have been obtained by the following procedure:[29] First, a Hartree−Fock calculation is carried out for the dianion using only the polarized valence basis without the diffuse functions yielding a set of compact molecular orbitals (MO). Then the diffuse functions are symmetry adapted, orthonormalized, and added to the compact MO basis. The CI wavefunction is constructed from the closed-shell configuration, which puts all electrons into compact MOs of the polarized triple-ζ set, and all singly excited configurations, where in particular the single excitations into the diffuse orbitals describe the autodetachment process.

Using the CAP/CI approach and basis set described above, we obtain a resonance width of $\Gamma = 37$ meV, which translates into a lifetime of 9 fs. This is a short lifetime in the order of those of typical shape-type resonances. In ref 29 it is shown that for closed-shell resonances the lifetimes obtained from wavefunctions similar in quality to the present are very close to those obtained from more accurate multireference treatments including single and double excitations on top of all configurations employed here. Therefore, we are confident to predict a short lifetime on the order of 10 fs. Clearly, the only way to study the isolated Al_4^{2-} dianion experimentally is to use electron scattering techniques.

Let us note that recently several small dianions have been studied at storage rings.[33−36] Small dianions can only then be stable, or at least have a long lifetime, if the excess electrons can separate and localize on at least two substructures with a large local electron affinity.[31] For example, CO_3^{2-} is predicted to have a much longer autodetachment lifetime in the ps range,[30] and the isoelectronic LiF$_3^{2-}$ dianion is stable with respect to electron autodetachment.[37]

Interestingly, the lifetime of Al$_4^{2-}$ is very similar to that of the cyclooctatetraene dianion which has been predicted to be 6 fs. Both systems are generally referred to as being aromatic; however, the Coulomb repulsion of the excess electrons dominates these species. The short lifetime suggests that the bound-state description of the dianion is problematic, even though a time-independent approximation to the full problem has been used successfully for other systems (cf. refs 38 and 39).

III. Bound-State Calculations

Both the simple DFOSA approach as well as more sophisticated CAP/CI calculations indicate that the Al$_4^{2-}$ dianion is a short-lived species. In this section we investigate the instability of the bound-state solution with respect to admixture of continuum solutions. This is done by observing the influence of basis set diffuseness on the ground-state energy both at the complete active space self-consistent field (CASSCF) and generalized active space configuration interaction (GASCI) levels of theory. To further strengthen our arguments, we demonstrate the dramatic basis set dependence of nuclear magnetic shieldings of Al$_4^{2-}$ in CASSCF calculations. Shieldings as well as related magnetic properties (like nucleus-independent chemical shieldings (NICS)[40] or magnetically induced ring currents[4−6]) have played an important role in the assessment of the system's aromaticity.

A. Computational Methods. *1. Electronic Structure of the Molecule.* The full symmetry group of the Al$_4^{n-}$ ($n = 2, 1$) molecules is D_{4h}. All calculations were carried out in the D_{2h} subgroup, and in the following discussion, orbitals and states will be named according to irreducible representations (irreps) within this subgroup.

The ground-state of the dianion is a closed-shell ^1A_g state with electron configuration $(1-7)a_g^2$, $(1-5)b_{1u}^2$, $(1-5)b_{2u}^2$, $(1-5)b_{3g}^2$, $(1-2)b_{3u}^2$, $1b_{1g}^2$, $1b_{2g}^2$, $1a_u^2$.[41] A bond length of 2.598 Å was used throughout, which was obtained[42] at the B3-LYP/TZVPP level of theory[43−46] and agrees well with the literature values.[1−3,7]

The valence space of the dianion is formed by 3s and 3p orbitals at MO energies from −8 to +1.7 eV ($(5-7)a_g$, $5b_{1u}$, $5b_{2u}$, $5b_{3g}$, $2b_{3u}$), as shown in Table I. Both highest-lying occupied MOs ($7a_g$ and $2b_{3u}$) are strongly antibonding. Within the one-electron picture it is therefore expected that the dianion will decay by emitting an electron from one of these orbitals yielding the monoanion in a $^2B_{3u}$ or ^2A_g state. We considered both possibilities since the energies of these two states are relatively close and in fact their energetic ordering may change from uncorrelated to correlated calculations (see section IIIB). A change in the order of orbital energies was not observed when going from the dianion to the monoanion.

Symmetry conservation demands that the direct product of the irreps of the free-electron wave and the orbital from which the electron is removed is totally symmetric (because Al$_4^{2-}$ has a totally symmetric ^1A_g ground state). Within the D_{2h} group this is only possible if the outgoing electron wave is of the same symmetry as the orbital from which it emerges. In order to describe the outgoing single electron, a multireference or open-shell description is essential, because in a single-determinant closed-shell reference wave function all orbitals are forced to be doubly occupied. The situation for the isolated dianion is thus considerably different from that of calculations including counterions, where no strong multireference behavior was observed.[2] The most important active MOs for describing the decay of the dianions will be the highest-lying MOs of a_g and $b_{1,2,3u}$ symmetry; this choice of active space covers those MOs relevant to the decay process and those required for describing the most important interacting electronic configurations.

TABLE 1: Electron Configuration and Description of MOs for the Al$_4^{2-}$ Dianion (aTZVPP Basis)[a]

Region	a_g	b_{1u}	b_{2u}	b_{3g}	b_{3u}	b_{1g}	b_{2g}	a_u
valence	7 +1.5 $3s, 3d$				2 +1.7 $3p_z$			
	6 +1.2 $3s, 3p_{x,y}$			5 +0.4 $3s$				
	5 −7.8 $3s$	5 −3.8 $3s$	5 −3.8 $3s$					
outer core	2 − 4	2 − 4	2 − 4	2 − 4	1	1	1	1
	−126 to − 80 $2s, 2p_{x,y}$				−80 $2p_z$			
core	1	1	1	1				
	−1584 $1s$							

[a] The first row within each block contains the ordinal number of each MO within its respective irreducible representation followed by its energy in the second row. In the third row, the AOs which mainly contribute to the MO are given. All energies are given in eV.

2. Basis Sets. It is well-known that basis sets of sufficient size need to be employed in order to achieve an appropriate description of angular and radial correlation. As such, basis sets of triple-ζ quality are a reasonable compromise between computational efficiency and accuracy: Basis sets of triple-ζ quality ensure in typical MRSDCI calculations that basis set errors are smaller than remaining correlation errors. Benchmark calculations on monoanions point out that diffuse functions are inevitable in the description of the diffusely bound outer electrons of these systems.[47] The latter is especially true for multiply charged anions (although no exhaustive systematic investigations on basis set requirements for dianions are known to the authors).

We employ here a basis set of TZVPP quality,[46] which was augmented by a set of diffuse (1s1p1d1f) functions in order to improve the description of the dianion's diffuse electron distribution. The orbital exponents of the additional functions are 0.02 (s), 0.01425 (p), 0.0365 (d), and 0.08 (f), respectively. They were taken from optimizations of the atomic electron affinity of the aluminum atom at CCSD(T) level with 11/12 correlated electrons in the neutral/anion species.[42] The basis set, which will be referred to as aTZVPP in the following, reproduces the experimental atomic electron affinity to within 0.014 eV at the CCSD(T) level, so that it is reasonably balanced as far as size and accuracy are concerned.

Starting with the aTZVPP basis, we investigated the admixture of continuum solutions to the bound-state wave function by making the basis functions more and more diffuse. To describe the outgoing s and p wave, a diffuse s or p Gaussian function was added, respectively. These additional functions were centered on a ghost atom in the middle of the Al$_4^{2-}$ ring and their exponents were varied from 0.01 to 0.00001. The addition of very diffuse ghost orbitals (small exponents) correspond to outgoing low-energy electron wave packets, whereas more compact orbitals describe wave packets of higher energies.

3. Correlation Approaches. We investigate the stability and influence of diffuse basis functions on the wave function of the dianion using CASSCF and GASCI calculations. The CASSCF calculation is expected to describe the decay process qualitatively, whereas GASCI is employed to include dynamic correlation effects.

a. General Remarks. Correlated electronic wave functions are today often obtained by refined grouping and occupation of active orbital spaces. At the orbital optimization level, this can be carried out by means of the restricted active space (RAS) SCF procedure, as, e.g., implemented in the MOLCAS package.[48] A complete active space (CAS) SCF wave function is but a special case of this procedure, where the correlation treatment is restricted to a single active space in which a full configuration interaction (FCI) calculation is carried out.

The best possible generalization of this model is to employ an arbitrary number of active spaces and to allow arbitrary occupations of these (limited only by the Pauli principle).[49] It has been implemented in the context of CI optimizations (GASCI) in the LUCITA[50] module of the MOLCAS package and allows for the most flexible definition of the correlated wave function. We exploit these ideas in our study and report details in the following subsection.

b. Computational Details. A (4 electrons,10 orbitals)-CAS was chosen for a qualitative description of the decay process under emission of an s and p wave and to obtain a suitable reference wave function for the subsequent dynamically correlated calculations. Included in this CAS were the most important MOs for the decay process: The two highest-lying occupied molecular orbitals (MOs) and the corresponding ghost orbital of each irrep, that is two orbitals of a_g symmetry (s) and two of b_{3u} symmetry (p_z). Additionally, three orbitals of b_{1u} and b_{2u} symmetry were included in order to allow for decay in form of p_x or p_y waves. For the latter irreps, three MOs have to be included in the CAS space, because the first excited MO in these irreps does not comprise the ghost orbital.

GASCI calculations were performed to investigate the effects of dynamic electron correlation. To include diffuse ghost orbitals in irreps b_{1u} and b_{2u} in the GA space while keeping it as small as possible, an orbital rotation between MOs 7 and 8 was carried out in these irreps such that only two MOs of these irreps had to be included in the multireference description. Core and outer core electrons (1s up to 2p) were gathered in spaces GAS0 and GAS1, respectively, and not correlated due to high computational demands. The valence shell was split into two active spaces: GAS2 ($1a_g$, $1b_{1u}$, $1b_{2u}$,$1b_{3g}$) and GAS3 ($3a_g$, $1b_{1u}$, $1b_{2u}$, $2b_{3u}$). Double excitations were allowed from GAS2. For GAS3, which is the most important space for the description of the ‘decay process’, a minimum of 4 and a maximum of 8 electrons in 7 MOs was allowed. The remaining GAS4 space comprises all virtual orbitals. A table of the spaces is given in Table 2.

Our definition of the model space corresponds to a multireference SD CI expansion with a hole reference space limited to a maximum of 2 holes and a combined CAS reference space. Determinants with 4 electrons in GAS3 represent double excitations from the multireference space into the virtual space, whereas such with 8 electrons in GAS3 represent double excitations from the GAS2 orbitals *into* the valence orbitals without excitations into the virtual space. These latter determinants are very few compared to the total number of determinants. The total expansion lengths amounted to more than 300 million Slater determinants. The program suite MOLCAS 5[48] was used for all energy calculations reported in this section and scalar-relativistic corrections within the Douglas-Kroll-Hess approach[51] were employed throughout.

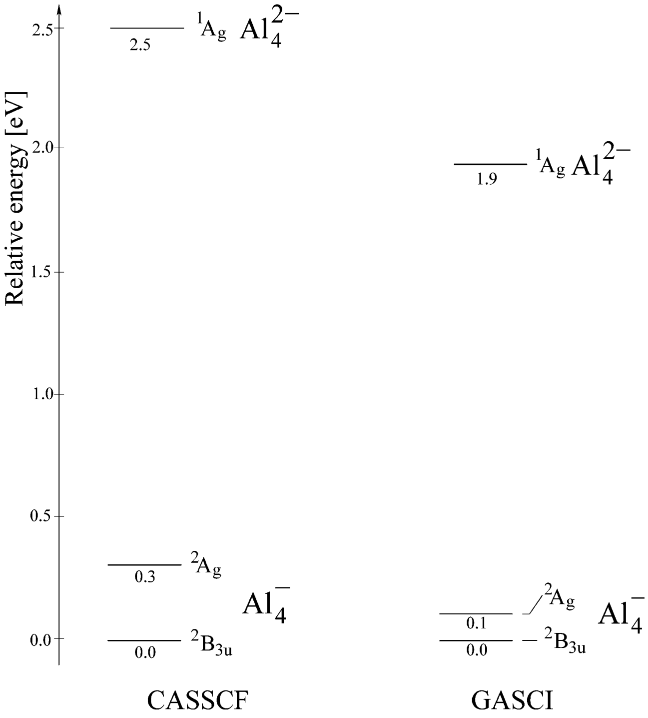

Figure 2. Relative energies of Al_4^{2-} and Al_4^- states calculated at CASSCF and GASCI levels of theory.

4. Computational Details for Calculation of Nuclear Magnetic Shieldings. The ^{27}Al nuclear magnetic shieldings of the Al_4^-(^2A_g,$^2B_{3u}$) and Al_4^{2-}(^1A_g) anions were calculated at the CASSCF level with the same choice of basis sets (aTZVPP+ghost) and correlation spaces as described above. We used the Dalton program package[52] and chose the center of mass as gauge origin. In addition, we calculated the shieldings using the cc-pV(2−4)Z,[53] aug-cc-pV(2−3)Z,[54] and TZVPP[46] basis sets to check whether similar effects can be observed with standard basis sets. As a side remark we point out that our open-shell calculations yield only the orbital response to the magnetic field and not all (experimentally measurable) contributions to the paramagnetic chemical shift. This should not, however, affect the qualitative results of our shielding calculations.

B. Results and Discussion. *1. Impact at the CASSCF Level.* The relative CASSCF energies of the monoanion in the ^2A_g and $^2B_{3u}$ states are 0.3 and 0.0 eV, respectively. A diagram of the energy levels is shown in Figure 2. Figure 3, panels a and b, shows the dianion CASSCF energies after addition of increasingly diffuse s and p ghost orbitals. The following trends can be observed: The dianion’s relative CASSCF energy is lowered from 2.5 to 0.5 eV for an outgoing s wave and to 0.1 eV for a p wave under addition of increasingly diffuse ghost orbitals. That is, with diffuse ghost orbitals the monoanion energies are obtained. This supports the point of view presented in the introduction, namely, that depending on basis set diffuseness the wave function undergoes a change from that of Al_4^{2-} to $Al_4^- + e^-$.

From the fact that rather small changes in the energy are observed when adding moderately diffuse functions it could be concluded that one has to go to very diffuse functions until the dianionic wave function is changed appreciably. The weights

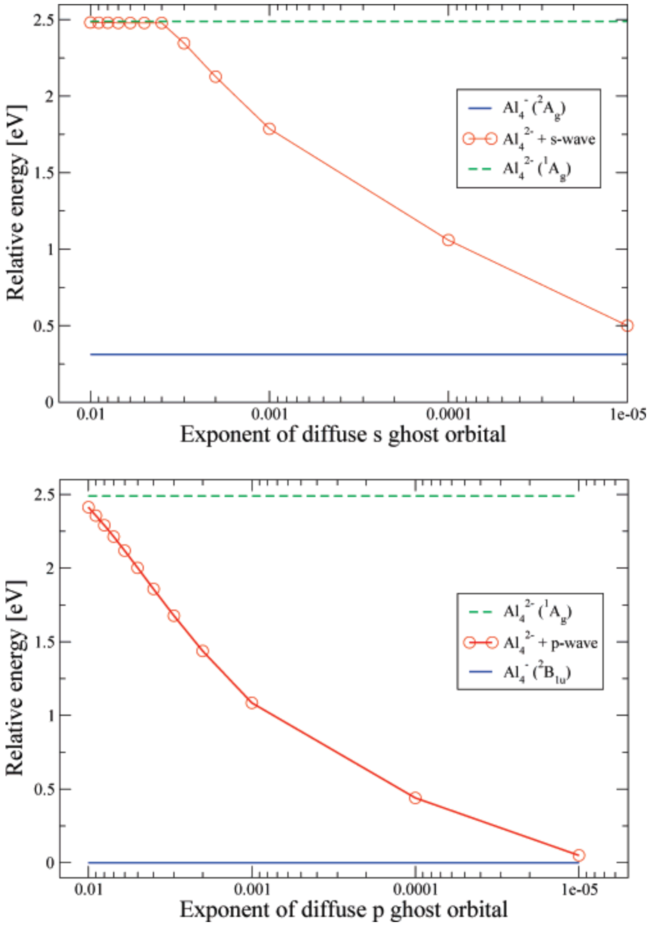

Figure 3. Dependence of CASSCF energies on basis set diffuseness with (a) s-type diffuse ghost orbital and (b) p-type diffuse ghost orbital added.

of open-shell continuum determinants, however, show that there is considerable influence of the continuum wave functions already at rather large ghost orbital exponents;[55] that is, the continuum wave function has a weight of approximately 18% for a diffuse s ghost orbital of exponent 0.01, and for a p ghost orbital of exponent 0.01 the continuum wave function admixture is even co-dominant with a weight of 49%.[55] The admixture of continuum wave functions is therefore much stronger than anticipated from the lowering of the energy. This can be understood by keeping in mind that a large-exponent Gaussian function corresponds to a detached electron wave packet of high energy. The stability of the energy with respect to adding more diffuse basis functions is therefore no reliable criterion for the stability of the wave function.

2. Impact at the GASCI Correlated Level. Essentially the same trends can be observed at the GASCI level, as shown in Figures 4, panels a and b. The monoanion ground state is $^2B_{3u}$, and the first excited-state is ^2A_g with relative energies of 0.0 and 0.1 eV, respectively (see Figure 2). Compared to the CCSD(T) results from ref 7 the ordering of the two states is inverted.

Like in the CASSCF case, the relative GASCI energy is lowered dramatically from 1.9 to 0.2 eV (s detachment) and to 0.3 eV (p detachment) under addition of diffuse ghost orbitals: The dianion wave function becomes more and more like that of $Al_4^- + e^-$ until at small orbital exponents (<0.001 for s wave and <0.01 for p wave) the energy essentially resembles that of the lowest-lying continuum solutions. We remark that already by going from the TZVPP to the aTZVPP basis and adding a diffuse p orbital of exponent 0.01 the energy is lowered significantly (0.5 eV) toward the monoanion energy.

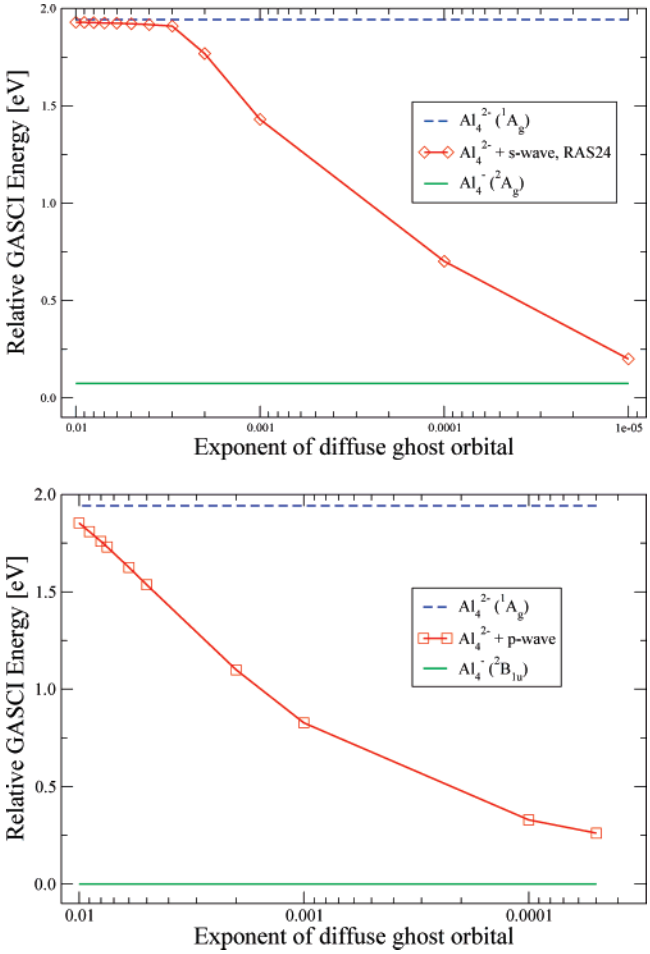

Figure 4. Dependence of GASCI energies on basis set diffuseness with (a) s-type diffuse ghost orbital and (b) p-type diffuse ghost orbital added.

The weights of monoanion-like determinants are very similar to those at the CASSCF level;[55] they increase from 16% to 92% (s detachment) and from 45% to 98% (p detachment) under addition of diffuse basis functions. Again, the admixture of continuum solutions is much stronger than anticipated from the energy alone. In contrast to the CASSCF calculation, the influence of monoanion determinants grows slightly more rapidly with basis set diffuseness (of s ghost orbitals) at this level of correlation. Significant admixture of continuum wave functions to the dianion wave function is observed already at relatively large orbital exponents: The p scattering solution has a weight of 45% at an orbital exponent of 0.01 for the p ghost orbital.

3. Impact on Nuclear Magnetic Shieldings. Our findings for nuclear magnetic shieldings are very similar to those for the CASSCF and GASCI energies and wave functions. While the chemical shieldings of Al_4^- in the ^2A_g and $^2B_{3u}$ states remain essentially constant when adding more diffuse basis functions (369.4−369.3 and 278.6−278.9 ppm, respectively), the shieldings of the dianion Al_4^{2-} vary considerably depending on the diffuse functions added (see Figure 5).

Adding diffuse s ghost orbitals increases the shieldings from initially 289.1 to 361.9 ppm, which is essentially the same as for the monoanion in ^2A_g state. With diffuse p orbitals, the shieldings can be lowered down to 278.8 and even further to 225.3 ppm, which is lower than the monoanion $^2B_{3u}$ shieldings. With a spread of 136.6 ppm (up to 61% of dianion's lowest shieldings), almost arbitrary results can be obtained depending on the basis set.

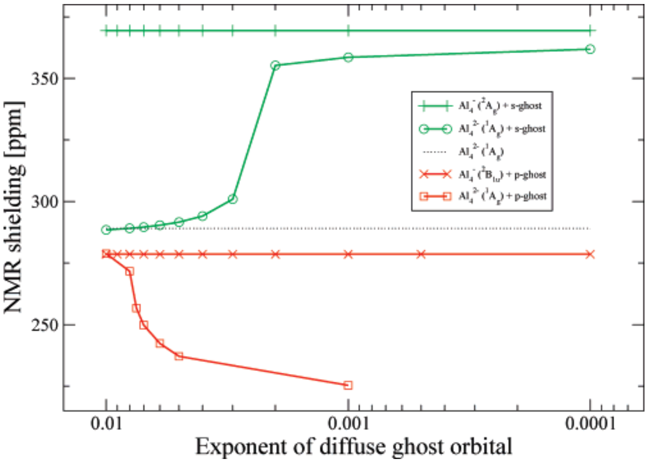

Figure 5. Dependence of nuclear magnetic shieldings on basis set diffuseness at CASSCF level.

TABLE 2: Number of Orbitals in Each Generalized Active Space (GAS) for the GASCI Calculation and Minimum/Maximum Electron Occupation for Each[a]

GAS space	a_g	b_{1u}	b_{2u}	b_{3g}	b_{3u}	b_{1g}	b_{2g}	a_u	N_{min}	N_{max}
GAS0	1	1	1	1	0	0	0	0		
GAS1	3	3	3	3	1	1	1	1	32	32
GAS2	1	1	1	1	0	0	0	0	38	40
GAS3	3	1	1	0	2	0	0	0	44	46
GAS4	28	29	29	30	15	17	17	17	46	46

[a] Electron Numbers are Cumulative.

TABLE 3: Excitation Energies (in eV) for Lowest-Lying States Contributing to Orbital Zeeman Term to First-Order Calculated at (4,14)-CASSCF/aTZVPP Level[a]

	excited state			shielding		
basis	B_{1g}	B_{2g}	B_{3g}	total	dia	para
aTZVPP+p(0.001)	−0.02	−0.02	2.44	225.3	844.4	−619.0
aTZVPP+p(0.007)	0.52	0.52	1.30	249.8	845.4	−595.6
aTZVPP+p(0.008)	0.61	0.61	1.30	271.7	845.4	−544.5
aTZVPP+p(0.01)	0.83	0.83	1.29	278.8	844.6	−565.8
aTZVPP	0.93	0.93	1.27	289.1	843.7	−554.6
aTZVPP+s(0.01)	0.89	0.89	1.31	288.5	844.0	−555.5
aTZVPP+s(0.003)	1.14	1.14	1.43	301.0	843.6	−542.6
aTZVPP+s(0.002)	1.49	1.49	1.12	355.3	842.4	−487.1
aTZVPP+s(0.001)	2.23	2.23	1.09	355.3	842.4	−487.1

[a] Diamagnetic and paramagnetic contributions to shieldings (in ppm) are given for comparison.

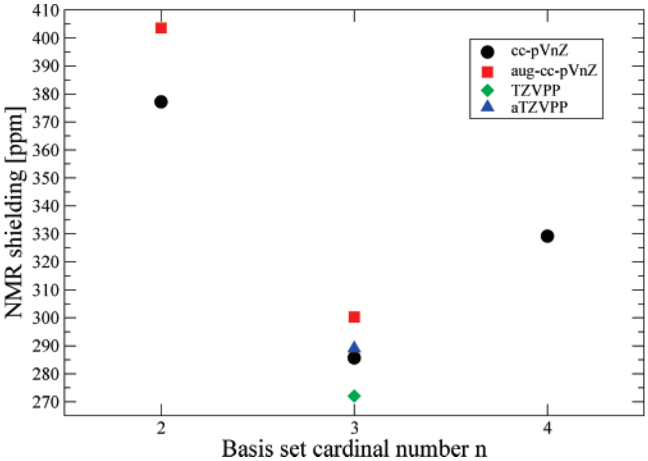

Figure 6. Nuclear magnetic shieldings at CASSCF level with some standard basis sets.

Interestingly, the effects of adding s and p ghost orbitals are opposite in sign. While the s ghost orbitals lead to increased shielding, p orbitals result in a deshielding of the nuclei. In Table 3 a decomposition into paramagnetic (negative) and diamagnetic (positive) contributions is presented. It can be seen that the diamagnetic contribution remains relatively constant, whereas the paramagnetic contribution varies strongly with the spatial extent of the basis set. This can be rationalized, e.g., by considering the sum-over-states expression for the shieldings and looking at the symmetry properties of low-lying excited states (cf. ref 56 for a similar approach in the context of magnetically induced ring currents; see also ref 57 for additional remarks).

The leading contribution to paramagnetic deshielding stems from the orbital Zeeman term, whose operator transforms like a rotation ($B_{1,2,3g}$ irreps within the D_{2h} group). Due to symmetry considerations, the lowest-lying $B_{1,2,3g}$ states are expected to give rise to the leading-order contributions to paramagnetic deshielding. In Table 3, a very nice agreement between excitation energies for the lowest-lying $B_{1,2g}$ states and paramagnetic contributions can be observed. It is found that a lowering of the excitation energy in symmetries $B_{1,2g}$ coincides with stronger paramagnetic deshielding, whereas an increase in the excitation energy corresponds to weaker paramagnetic contributions. On the other hand, the excitation energies for the lowest-lying B_{3g} state remain almost constant (except for very diffuse s and p functions). We therefore conclude that the leading-order contributions to the paramagnetic deshielding stem from interactions with low-lying $B_{1,2g}$ states, whose energies relative to the A_g ground state are strongly dependent on the choice of basis set.

In the light of the above investigation it is not surprising that the shieldings exhibit a stronger dependence on basis set diffuseness than energies. This was also already anticipated in section IIIB1, because the relative stability of the energy is misleading and energy derivatives and response properties depend more critically on the wave function. It is remarkable that, like for the energy calculations, already moderately diffuse p functions ($\alpha \approx 0.01$) have a strong influence on the shieldings. Considering results for some common basis sets (Figure 6), one can see that (a) no convergence of the results with basis set cardinal number can be found and (b) depending on the basis set essentially any result ranging from that of the ^2A_g to that of the $^2B_{1u}$ state can be produced. For example, the TZVPP results are 131.5 ppm lower than the aug-cc-pVDZ results.

Finally, we note that our CASSCF NMR shieldings are close to those obtained by Juselius et al.[3] at the CCSD(T) level of theory. The correct description of *static* electron correlation is essential here for qualitatively correct results, which is modeled by higher-order excitations in the CCSD(T) approach. This is probably the reason for the failure of MP2 in ref 3 in obtaining correct NMR shieldings for Al_4^{2-}.

C. Conclusions from Bound-State Calculations. The admixture of scattering solutions to the bound-state wave functions is non-negligible for s-wave scattering and becomes very pronounced for p-wave scattering already for moderately diffuse orbital exponents of 0.01 (p detachment). This is seen both in the CASSCF and GASCI energies and very strongly in the weights of continuum wave functions.

It is immediately clear that admixture of continuum solutions to the bound-state wave function may have significant influence on molecular properties like, e.g., nuclear magnetic resonance parameters, since the response of a free electron to an external magnetic field can be very different from that of an electron confined within a molecule. For the nuclear magnetic shieldings considered here the results depend dramatically (up to 136.6 ppm) on the presence of diffuse functions in the basis set and

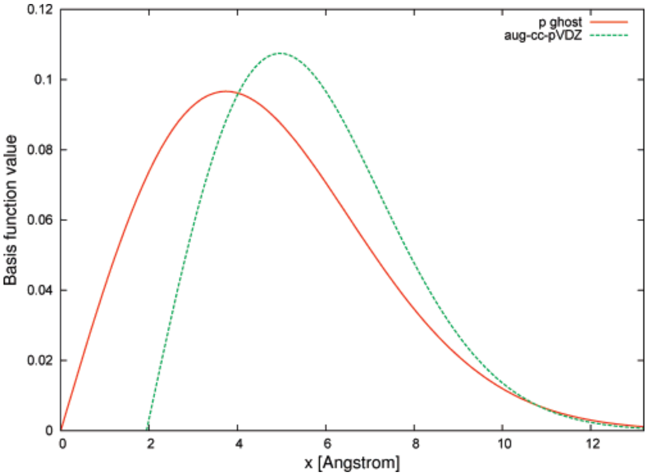

Figure 7. Comparison of diffuseness of a p-ghost orbital used in this study and that of a standard aug-cc-pVDZ p orbital (exponents 0.01 and 0.0153, respectively).

the balance between functions of different angular momenta (which even lead to effects of opposite sign).

We note that the functions used in our aTZVPP+ghost calculations have smaller exponents (0.01 and smaller) than those used in standard augmented basis sets (e.g., aug-cc-pV*n*Z series: p exponents 0.0153 and smaller). However, in the present study the diffuse functions were centered in the middle of the Al_4 ring, while the standard basis sets are atom-centered and therefore the spatial extent of, e.g., the augmentation functions of aug-cc-pVDZ are comparable to our basis (see Figure 7). The latter are known to be necessary for an adequate description of anionic systems. Therefore, it is not surprising that our findings from section IIIB3 were qualitatively reproduced by calculations with standard basis sets like the aug-cc-pV*n*Z series, where a dramatic dependence of the results on basis set diffuseness was observed.

IV. Conclusions

We have investigated the height of the repulsive Coulomb barrier and the resonance lifetime of the isolated Al_4^{2-} dianion (section II). Within a simple DFOSA approach, the RCB height can be estimated to be 2.7 eV, which is about 0.5 eV above the HOMO energy. A semiclassical WKB estimate yields a very short lifetime on the order of the time a valence electron needs to transverse the molecule's ring. For a more reliable estimate the CAP/CI method was employed, which confirmed the DFOSA estimate and resulted in a short lifetime of 9 fs. From these results we conclude that the only experimental technique to study the isolated Al_4^{2-} is electron scattering.

The limits of the time-independent approximation, i.e., the bound-state approach, for the description of the system were studied in section III. To this end, the impact of basis set diffuseness on CASSCF and GASCI energies and wave functions was investigated using an augmented TZVPP basis and the cc-pV*n*Z and aug-cc-pV*n*Z series of basis sets. It was shown that there is significant admixture of continuum solutions to the bound-state wave function of the dianion already for moderately diffuse basis functions. Depending on the basis set diffuseness, almost any energy can be calculated in the range from that of Al_4^{2-} (^1A_g) to Al_4^- ($^2B_{3u}$, ^2A_g). A similar instability and arbitrariness in the results was observed for nuclear magnetic shieldings, which have played an important role in the literature for the characterization of the molecule's aromaticity.[1−6,10−13,58]

Bound-state calculations therefore face the following dilemma: Either diffuse functions are included in the basis for an adequate description of the dianion's electron distribution or one restricts the basis to compact functions to prevent admixture of continuum solutions. Our study clearly demonstrates that the bound-state description of the isolated Al_4^{2-} is ill defined already for basis sets with moderately diffuse augmentation functions, and that the numerical results depend dramatically on the fortuitous balance between compact and diffuse basis functions. To put it in the words of Ahlrichs from his investigation of the Hartree−Fock problem for unstable dianions:[19] "Conventional HF treatments ... may yield results which are far from the HF limit and are more or less artefacts of the chosen basis set.''

Let us finally note that our statements apply only to the isolated dianionic species. If it is stabilized by a positively charged counterion, the system is stable with respect to electron detachment and bound-state approaches are well-defined.[1,2] In fact, recent studies of Islas et al.[59] show that the counterions have an influence on the chemical structure and that they should always be included in calculations. This is another way of stating that results for metastable systems should be approached with caution.

Acknowledgment. The authors are indebted to Christel M. Marian for helpful discussions and for providing computing time on the local linux cluster. We also thank A. I. Boldyrev for providing data from his calculations and Juha Vaara for helpful discussions on NMR calculations. D.S.L. is grateful for a Kekulé fellowship of the German "Fonds der Chemischen Industrie".

References and Notes

(1) Li, X.; Kuznetsov, A. E.; Zhang, H.-F.; Boldyrev, A. I.; Wang, L.-S. *Science* **2001**, *291*, 859.
(2) Boldyrev, A. I.; Kuznetsov, A. E. *Inorg. Chem.* **2002**, *41*, 532.
(3) Jusélius, J.; Straka, M.; Sundholm, D. *J. Phys. Chem. A* **2001**, *105*, 9939−9944.
(4) Fowler, P. W.; Havenith, R. W. A.; Steiner, E. *Chem. Phys. Lett.* **2002**, *359*, 530.
(5) Fowler, P. W.; Havenith, R. W. A.; Steiner, E. *Chem. Phys. Lett.* **2001**, *342*, 85.
(6) Havenith, R. W. A.; Fowler, P. W. *Phys. Chem. Chem. Phys.* **2006**, *8*, 3383.
(7) Zhan, C.-G.; Zheng, F.; Dixon, D. A. *J. Am. Chem. Soc.* **2002**, *124*, 14795−14803.
(8) Santos, J. C.; Andres, J.; Aizman, A.; Fuentealba, P. *J. Chem. Theor. Comp.* **2005**, *1*, 84.
(9) Santos, J. C.; Tiznado, W.; Contreras, R.; Fuentealba, P. *J. Chem. Phys.* **2004**, *120*, 1670.
(10) Havenith, R. W. A.; Fowler, P. W.; Steiner, E.; Shetty, S.; Kanhere, D.; Pal, S. *Phys. Chem. Chem. Phys.* **2004**, *6*, 285.
(11) Chen, Z.; Corminboeuf, C.; Heine, T.; Bohmann, J.; Schleyer, P. v. R. *J. Am. Chem. Soc.* **2003**, *125*, 13930.
(12) Lin, Y.-C.; Jusélius, J.; Sundholm, D.; Gauss, J. *J. Chem. Phys.* **2005**, *122*, 214308.
(13) Boldyrev, A. I.; Wang, L.-S. *Chem. Rev.* **2005**, *105*, 3716.
(14) Chattaraj, P. K.; Roy, D. R.; Subramanian, V. *J. Phys. Chem.* **2005**, *109*, 9590.
(15) Datta, A.; Pati, S. K. *J. Chem. Theory Comput* **2005**, *1*, 824.
(16) Jiménez-Halla, J. O. C.; Matito, E.; Robles, J.; Solá, M. *J. Organomet. Chem.* **2006**, *691*, 4359.
(17) Havenith, R. W. A.; Fowler, P. W. *Phys. Chem. Chem. Phys.* **2006**, *8*, 3383.
(18) Mallajosyula, S. S.; Datta, A.; Pati, S. K. *J. Phys. B* **2006**, *110*, 20098.
(19) Ahlrichs, R. *Chem. Phys. Lett.* **1975**, *34*, 570.
(20) Sommerfeld, T.; Tarantelli, F.; Meyer, H.-D.; Cederbaum, L. S. *J. Chem. Phys.* **2000**, *112*, 6635−6642.
(21) Dreuw, A.; Cederbaum, L. S. *Phys. Rev. A* **2001**, *63*, 049904.
(22) Dreuw, A.; Cederbaum, L. S. *Chem. Rev.* **2002**, *102*, 181.
(23) For the larger TZVPP and aTZVPP basis sets employed in the succeeding sections, HOMO energies of 1.7−2.4 eV are obtained.
(24) Messiah, A. *Quantum Mechanics*, 2nd ed.; Walter de Gruyter: Berlin, 1991; Vol. 1.
(25) Sommerfeld, T.; Riss, U. V.; Meyer, H. D. *J. Phys. B* **1998**, *31*, 4107.

(26) Sommerfeld, T.; Santra, R. *Int. J. Quantum Chem.* **2001**, *82*, 218.

(27) Jolicard, G.; Austin, E. J. *Chem. Phys.* **1985**, *103*, 295.

(28) Riss, U. V.; Meyer, H. D. *J. Phys. B* **1993**, *26*, 4503.

(29) Sommerfeld, T.; Tarantelli, F. *J. Chem. Phys.* **2000**, *112*, 2106.

(30) Sommerfeld, T. *Phys. Rev. Lett.* **2000**, *85*, 956.

(31) Sommerfeld, T. *J. Am. Chem. Soc.* **2002**, *124*, 1124.

(32) Dunning, T. H. *J. Chem. Phys.* **1971**, *55*, 716.

(33) Pedersen, H. B.; Djuric, N.; Jensen, M. J.; Kella, D.; Safvan, C. P.; Schmidt, H. T.; Vejby-Christensen, L.; Andersen, L. H. *Phys. Rev. A* **1999**, *60*, 2882.

(34) Pedersen, H. B.; Bilodeau, R.; Jensen, M. J.; Makassiouk, I. V.; Safvan, C. P.; Andersen, L. H. *Phys. Rev. A* **2001**, *63*, 032718.

(35) Seiersen, K.; Bak, J.; Bluhme, H.; Jensen, M. J.; Nielsen, S. B.; Andersen, L. H. *Phys. Chem. Chem. Phys.* **2003**, *5*, 4814.

(36) El Ghazaly, M. O. A.; Svendsen, A.; Bluhme, H.; Nielsen, S. B.; Andersen, L. H. *Chem. Phys. Lett.* **2005**, *405*, 278.

(37) Scheller, M. K.; Cederbaum, L. S. *J. Phys. B* **1992**, *25*, 2257.

(38) Pyykkö, P.; Zhao, Y. *Mol. Phys.* **1990**, *70*, 701 and references therein.

(39) Pyykkö, P.; Zhao, Y. *J. Phys. Chem.* **1990**, *94*, 7753 and references therein.

(40) Chen, Z.; Heine, T.; Schleyer, P. v. R.; Sundholm, D. *Comp. Chem. Annex* **2004**, page *395*.

(41) All electron configurations were confirmed by carrying out ground state calculations in C_1 symmetry.

(42) Lambrecht, D. S. Diploma thesis, Mathematisch-Naturwissenschaftliche Fakultät; Heinrich-Heine-Universität Düsseldorf: Düsseldorf, Germany, 2003.

(43) Lee, C. T.; Yang, W. T.; Parr, R. G. **1988**, *37*, 785.

(44) Becke, A. D. *J. Chem. Phys.* **1993**, *98*, 5648.

(45) Kohn, W.; Becke, A. D.; Parr, R. G. *J. Phys. Chem.* **1996**, *100*, 12974.

(46) Schäfer, A.; Huber, C.; Ahlrichs, R. *J. Chem. Phys.* **1994**, *100*, 5829.

(47) Dunning, T. H.; van Mourik, T.; Peterson, K. A. *Abstr. Am. Chem. Soc.* **2001**, *222*, 396.

(48) MOLCAS Version 5. Andersson, K.; Barysz, M.; Bernhardsson, A.; Blomberg, M. R. A.; Cooper, D. L.; Fleig, T.; Fülscher, M. P.; de Graaf, C.; Hess, B. A.; Karlström, G.; Lindh, R.; Malmqvist, P.-Å.; Neogrády, P.; Olsen, J.; Roos, B. O.; Sadlej, A. J.; Schütz, M.; Schimmelpfennig, B.; Seijo, L.; Serrano-Andrés, L.; Siegbahn, P. E. M.; Stålring, J.; Thorsteinsson, T.; Veryazov, V.; Widmark, P.-O. Lund University, Sweden, 2000.

(49) Fleig, T.; Olsen, J.; Marian, C. M. *J. Chem. Phys.* **2001**, *114*, 4775.

(50) LUCITA is a direct CI program written by J Olsen, *MOLCAS* interface by T. Fleig, 1999.

(51) Hess, B. *Phys. Rev. A* **1985**, *32*, 756.

(52) Dalton, a molecular electronic structure program, Release 1.2, written by Helgaker, T.; Jensen, H. J. Aa.; Joergensen, P.; Olsen, J.; Ruud, K.; Aagren, H.; Auer, A. A.; Bak, K. L.; Bakken, V.; Christiansen, O.; Coriani, S.; Dahle, P.; Dalskov, E. K.; Enevoldsen, T.; Fernandez, B.; Haettig, C.; Hald, K.; Halkier, A.; Heiberg, H.; Hettema, H.; Jonsson, D.; Kirpekar, S.; Kobayashi, R.; Koch, H.; Mikkelsen, K. V.; Norman, P.; Packer, M. J.; Pedersen, T. B.; Ruden, T. A.; Sanchez, A.; Saue, T.; Sauer, S. P. A.; Schimmelpfennig, B.; Sylvester-Hvid, K. O.; Taylor, P. R.; Vahtras, O. 2001.

(53) Woon, D. E.; Dunning, T. H., Jr. *J. Chem. Phys.* **1993**, *98*, 1358.

(54) Kendall, R. A.; Dunning, T. H., Jr. *J. Chem. Phys.* **1993**, *96*, 6796−6806.

(55) Supplementary data and information are available from the authors upon request.

(56) Steiner, E.; Fowler, P. W. *J. Chem. Phys.* **2001**, *105*, 9553.

(57) Kaupp, M. Interpretation of NMR chemical shifts. In *Calculation of NMR and EPR Parameters*; Kaupp, M., Bühl, M., Malin, V. G., eds.; Wiley-VCH: Weinheim, Germany, 2004; Chapter 18, pp 293−306.

(58) Boldyrev, A. I.; Wang, L.-S. *Chem. Rev.* **2005**, *105*, 3716.

(59) Islas, R.; Heine, T.; Merino, G. *J. Chem. Theory Comput.* **2007**, *3*, 775.